

Hybrid Air-Conditioning for Electric Vehicles by Combining a Heating and a Desiccant System

Uwe **Bau**, M.Sc, Dipl.-Ing. Heike **Schreiber**, Dr.-Ing. Franz **Lanzerath**,
Univ.-Prof. Dr.-Ing. André **Bardow**
Institute of Technical Thermodynamics, RWTH Aachen University, Germany

Summary

A key challenge for electric vehicles is the limited driving range by the batteries. Especially in winter, the driving range of electric vehicles is substantially reduced due to missing waste heat from the internal combustion engine. In this paper, a desiccant-assisted heating concept is proposed. In a dynamic simulation study, it is shown that the desiccant-assisted concept allows significantly reducing battery requirements for heating. The desiccant-assisted system actively removes water from the airflow allowing an increased air recirculation rate without risk of windshield fogging. The increased air recirculation rate results in a reduction of the electricity demand for heating up to 66 % compared to a conventional set-up without desiccant module and no air recirculation. Additionally, heat-up times at the beginning of a ride can be reduced significantly with the desiccant-assisted system: from 14 to 6 min for an ambient temperature of $-10\text{ }^{\circ}\text{C}$.

1 Introduction

Although the worldwide electric car stock exceeded 1 million in 2015, sales of electric cars have to grow substantially to meet the Paris Declaration on Electro-Mobility and Climate Change for 2030 [1]. One central issue still harming sales is the limited range due to expensive batteries [2]. Especially in winter, the driving range of electric vehicles is substantially reduced due to missing waste heat of the internal combustion engine [3]. For ambient temperatures of $0\text{ }^{\circ}\text{C}$, the driving range is reduced between 23 and 33 % and for $-20\text{ }^{\circ}\text{C}$, the range is even decreased by 50 % because of thermal needs [4–8]. Fig. 1 shows the heating and cooling demand of a typical car as a function of the ambient temperature compared to the average power used by the drivetrain. Additionally, the three modes of the heating, ventilation and air-conditioning (HVAC) system are illustrated: heating mode, dehumidification and re-heat mode, and cooling mode. In this study, we focus on the heating mode, since it has the largest impact on the driving range [4].

The heating demand has two causes of almost equal share [9, 10]: (1) heat losses at the car's envelope (windshield, roof, doors, ...) by radiation, conduction, and convection. These losses depend directly on the temperature difference between ambient air and cabin air ($T_{\text{ambient}} - T_{\text{cabin}}$). (2) Heating demand due to fresh outside air which has to be heated from T_{ambient} to T_{cabin} .

The resulting total heating demand can be lowered by mainly 3 measures:

First, lowering the cabin temperature T_{cabin} would decrease the heating demand caused by both reasons 1 and 2. Unfortunately, lowering the cabin temperature also reduces the thermal comfort of the passengers [11]. To overcome the reduction in thermal comfort, surface heating elements are suggested, e.g. seat heating or heating panels, which allow reducing cabin temperatures while maintaining thermal comfort [12].

Second, the insulation of the car's envelope could be increased. This measure would increase the thermal resistance of the car's envelope and thus, would lower the heating demand caused by reason 1. An increased insulation comes at the cost of additional weight [13].

Third, heating demand can be decreased by more than 50 % by recirculating the cabin air (cf. Fig. 1 top). Recirculation of cabin air is usually used in summer (cooling mode) to reduce the cooling demand. In winter, recirculation of cabin air is not used due to the risk of windshield fogging [14, 15]: Moisture which is produced by the passengers condenses at the cold surfaces of the windshield and door windows. This moisture can be removed from the cabin by fresh air with lower water content. Thus, air recirculation in winter is not possible due to the need of dry air: ambient air is dry but cold compared to cabin air. Atkinson et al. [16] suggest to use no air recirculation for ambient conditions below $T_{\text{ambient}} = 5\text{ }^{\circ}\text{C}$ to ensure safe operation due to moisture in the cabin.

If the air recirculation rate could be increased, the driving range of electric vehicles in winter would rise significantly (cf. Fig. 1 top). To allow high air recirculation rates in winter without the risk of fogging, we suggest adding a desiccant module to the HVAC system and combining it with active air recirculation rate control: The desiccant module is a thermochemical storage unit and allows for active dehumidification without the necessity of cooling down the air to the dew point. The active dehumidification enables higher air recirculation rates which correspond to a lower energy demand in heating and re-heat mode.

In Bau et al. [17], a preliminary analysis has suggested that significant energy reductions can be achieved in both heating and re-heat mode. In this study, a detailed model-based investigation is conducted of the heating mode, since the heating mode is responsible for the highest thermal demand and thus, the highest reduction in the driving range of an electric vehicle.

The paper is structured as follows: In Section 2, the HVAC set-up and the three investigated operating strategies are presented. In Section 3, dynamic models of the cabin, the HVAC system and the desiccant module are presented. In Section 4, the electrical energy demand for heating is quantified for the investigated operating strategies for ambient temperatures between $-20\text{ }^{\circ}\text{C}$ and $10\text{ }^{\circ}\text{C}$. Additionally, a detailed transient analysis of temperatures and control variables is shown for the case of $T_{\text{ambient}} = -10\text{ }^{\circ}\text{C}$. Finally, in Section 5, the results are summarized.

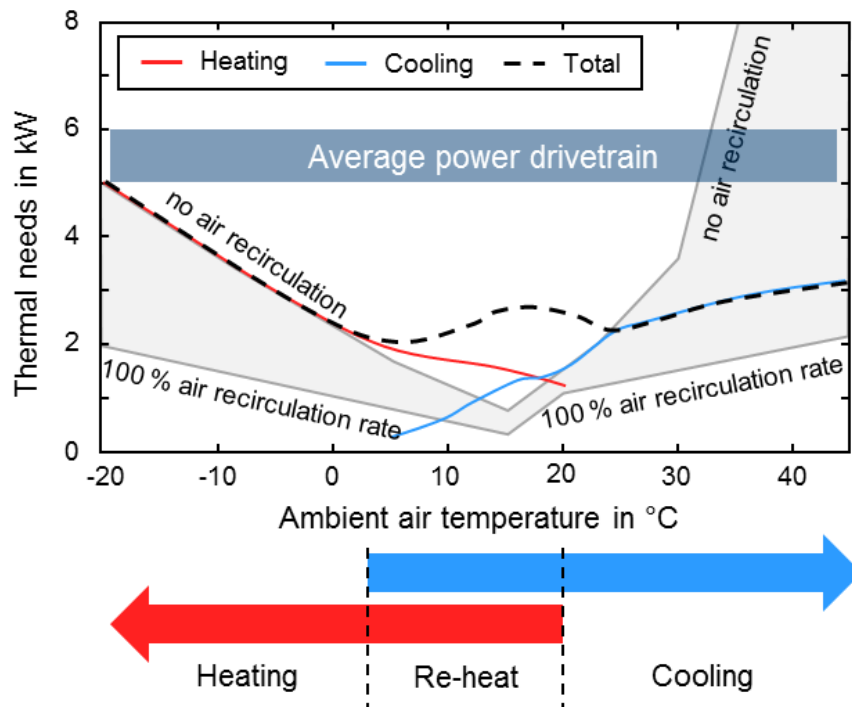


Fig. 1: Top: Energy demand for HVAC system and drivetrain: The energy demand for the HVAC system is based on a simulation study by Brèque and Nemer [10]. The average power for the drivetrain is derived from measurement data reported by Tober [4]. Bottom: Overview on heating and cooling modes based on ambient temperatures [18].

2 Desiccant-assisted heating concept

In this section, the concept of a desiccant-assisted heating system is presented. For this purpose, first the set-ups of the reference and the desiccant-assisted system are introduced. Based on these set-ups, three operating strategies are explained: (1) reference strategy (no air recirculation), (2) controlled air recirculation rate, and (3) desiccant-assisted controlled air recirculation rate. In Section 4, these three operating strategies are compared regarding energy demand and heat-up times. Finally, charging for the desiccant-assisted set-up is explained.

2.1 Set-ups

The reference set-up represents a state-of-art HVAC system for electric vehicles [5]. It includes an evaporator (AC-evap) of a compression chiller and a radiator (Fig. 2). The compression chiller may cool down and dehumidify the air. The following radiator heats the air before it enters the cabin. The heat for the radiator can be delivered by an electric positive-temperature-coefficient heater (PTC-heater) or by a heat-pump system. The air recirculation rate (ARR) can be varied between 0 % and 100 % by ventilation flaps.

The desiccant-assisted set-up suggested in this paper adds a desiccant module between the ventilation flaps and the evaporator at the inlet side (Fig. 2). The

desiccant module is a thermochemical storage unit which adsorbs water from the air until the module is saturated and needs to be recharged. Since adsorption is an exothermic process, heat is released and the airflow is heated. For charging, the desiccant module has to be dried: a hot airflow can be used to provide the necessary energy and to remove the water.

2.2 Operating strategies (cf. Figure 2)

In this sub-section, the three operating strategies studied are explained: (1) reference strategy (no air recirculation), (2) controlled air recirculation rate, and (3) desiccant-assisted controlled air recirculation rate. In Fig. 2, each operating strategy is illustrated in a Mollier-diagram.

2.2.1 Reference strategy (no air recirculation)

In the reference strategy, no air recirculation is applied, i.e. the air recirculation rate (ARR) is 0 %. In this operating strategy, ambient air is heated by the radiator (I) → (V). This operating strategy is commonly used below 5 °C to ensure safe operation without the risk of windshield fogging [16].

2.2.2 Controlled air recirculation rate

In the second operating strategy, the air recirculation rate is controlled, i.e. ambient air and cabin air are mixed (I) + (II) → (III). The mixing rate depends on the amount of moisture which has to be removed from the cabin: the more passengers are in the cabin, the more fresh ambient air is needed to remove the moisture. After mixing ambient and cabin air, the air is heated by the radiator (III) → (V) and blown into the cabin. To control the air recirculation rate and to ensure no windshield fogging, a humidity sensor is necessary inside the cabin.

2.2.3 Desiccant-assisted controlled air recirculation rate

In the third operating strategy, a desiccant module is used to actively remove moisture from the air. As in strategy 2, cabin air and ambient air are mixed (I) + (II) → (III). Afterwards, the air is actively dried by a desiccant module (III) → (IV). In this step, moisture is removed from the air and, at the same time, the air is heated by the desiccant module. Finally, the air is heated by a radiator (IV) → (V). Due to the desiccant module, higher recirculation rates are possible compared to strategy 2.

In principle, 3 control variables can be used for all three operating strategies: the air mass flow rate, the air recirculation rate (ARR), and the heat flow rate at the radiator. In the reference strategy, the air recirculation rate is fixed to ARR = 0 %. The control variables are also shown in Fig. 2.

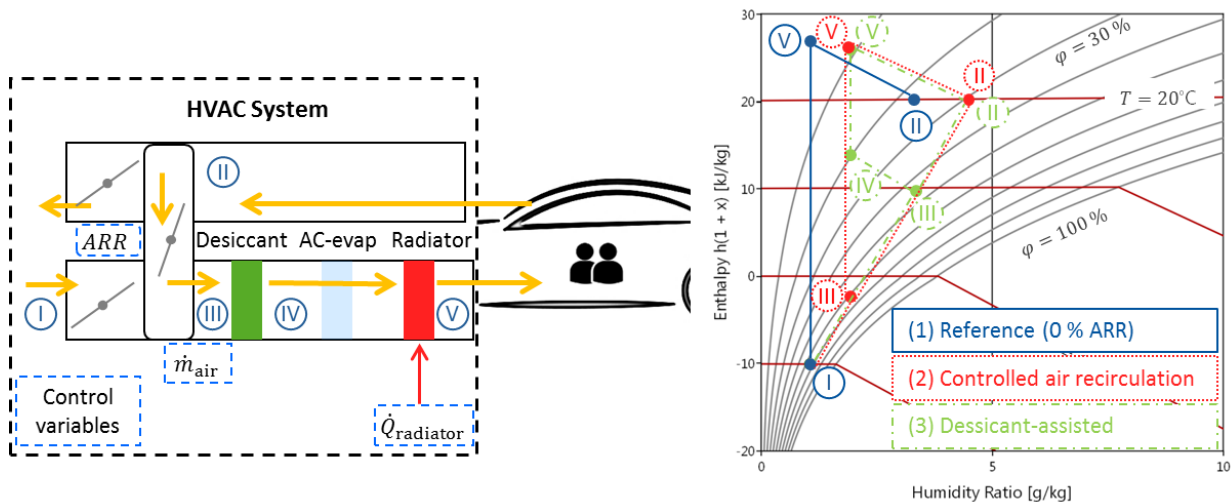


Fig. 2: Desiccant-assisted concepts for electric vehicle: Left: Air flow in heating, ventilation and air-conditioning (HVAC) system, consisting of desiccant module, AC-evaporator and radiator. Control variables are marked by dashed box: Air recirculation rate (ARR), Air mass flow rate (\dot{m}_{air}), and heat flow rate ($\dot{Q}_{\text{radiator}}$). Right: Mollier-diagram showing the states for the three operating strategies: (1) reference strategy (no air recirculation), (2) controlled air recirculation rate, and (3) desiccant-assisted controlled air recirculation rate.

2.3 Charging

In an electrical vehicle, the battery has to be charged. For the first two operating strategies, still only the batteries of the electric vehicle have to be charged. For the desiccant-assisted strategy, also the desiccant module needs to be charged. Charging the desiccant module means removing the adsorbed water from the desiccant module. This can be done by a hot airflow which is blown through the module. The hot airflow ($T_{\text{airflow}} \approx 90 \text{ }^\circ\text{C}$) provides the energy to dry the desiccant module. The airflow can be heated by either by a PTC-heater, or, if available, by a heat pump. Charging of the desiccant module is conducted when the electric vehicle is connected to the grid while the batteries are charged.

3 Dynamic models of cabin and HVAC system

To quantify the achievable reductions in energy demand with the desiccant-assisted heating system, dynamic models of the car cabin and the HVAC system are employed. Dynamic models are necessary to capture the transient conditions in a car. E.g., when starting a ride, the cabin air has to be heated from ambient temperature to set temperature. Fig. 3 shows the model structure. In the following, the sub-models for the cabin and the HVAC system are explained.

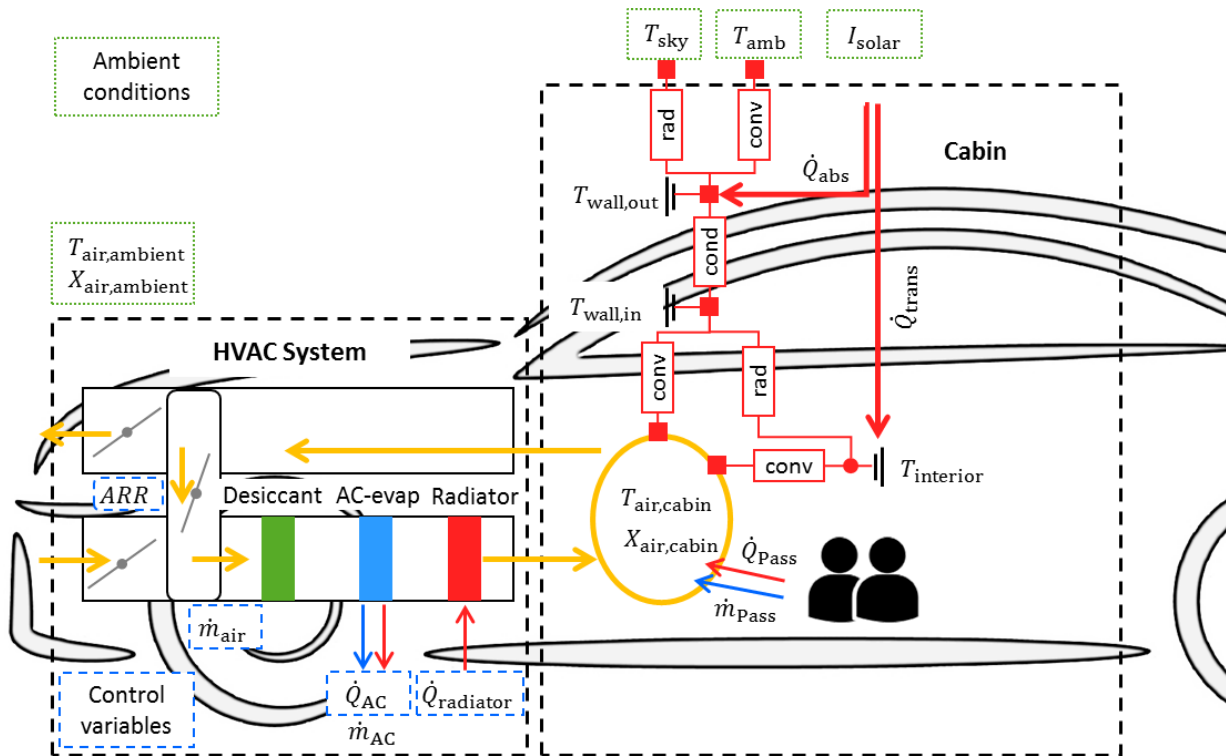


Fig. 3: Structure of dynamic model including sub-models of the cabin and the HVAC system. The HVAC system consists of models for the desiccant module, the AC-evaporator, the ventilation flaps, and the radiator. The cabin model consists of a thermal network considering radiation, conduction and convection, an air volume and a passenger model. Cabin and HVAC system are connected by the airflow (yellow arrows). Ambient conditions are indicated by green dotted boxes. Control variables are highlighted by blue dashed boxes.

3.1 Cabin

For the cabin, a one-zonal model is used, assuming perfect mixing of the cabin air. The cabin model consists of thermal resistances considering radiation, conduction and convection, an air volume, and a passenger model as described by Brèque and Nemer [10]. The cabin model allows determining the thermal demand depending on the ambient temperature and solar irradiation. Additionally, the temperatures at the inner surfaces (walls = windshield, roof, floor, doors...) are determined. This allows to calculate the local dew-point and to predict windshield fogging. With this information, the air recirculation rate can be controlled based on the local dew-point of the windshield.

3.1.1 Thermal network

The thermal network consists of heat capacities for the wall and the interior of the cabin. These thermal masses are connected by models for radiation, convection and conduction. The cabin walls (windshield, roof, floor, doors...) are modeled by two heat capacities connected by a model for conduction. The temperatures at the inside of the cabin surfaces, such as the windshield, are computed by the model, which allows predicting fogging.

For each heat capacity of the wall and the cabin interior, the energy balance is solved:

$$C \frac{dT}{dt} = \sum \dot{Q}$$

where C is the heat capacity, T is the temperature, t is the time and \dot{Q} are the heat flows.

The heat flows are determined by the following three equations.

In case of conduction:

$$\dot{Q}_{\text{cond}} = \frac{\lambda}{\delta} A (T_1 - T_2)$$

with λ as the thermal conductivity, δ as the walls thickness and A as the heat transfer surface.

In case of convection:

$$\dot{Q}_{\text{conv}} = \alpha A (T_1 - T_2)$$

with α as convective heat transfer coefficient and A as heat transfer area. Convective heat transfer coefficients on the inside and the outside are based on forced convection according to the international standard ISO 12837 [19].

In case of radiation:

$$\dot{Q}_{\text{rad}} = \epsilon \sigma A (T_1^4 - T_2^4)$$

with ϵ as the emissivity of the surface for long wave radiation and σ as the Stefan-Boltzmann constant.

Thermal conductivity and emissivity are based on material data of glass, steel and insulation material (polyurethane foam) respectively. All material data, such as thermal conductivity, density, or emissivity are based on the VDI-Wärmeatlas [20].

3.1.2 Cabin air

For the cabin air, the energy and mass balances are solved using a model for humid air. Thereby, information on cabin temperature and cabin humidity are obtained. The cabin temperature is used as control value for the heat flow of the radiator. The cabin humidity is used to determine the local dew-point at the windshield. The media model used for the humid air assumes an ideal mixture of two ideal gases: dry air and water with temperature dependent properties based on the VDI guideline 4670: Thermodynamic properties of humid air and combustion gases [21].

3.1.3 Passenger model

Passengers provide heat and moisture to the cabin air. In the model, we follow the guideline VDI 2078 [22]. Thus, passengers are modeled as a source of heat and moisture. The amount of produced heat and moisture depends on the number of passengers.

Solar irradiation is not considered in this study, since only heating cases are investigated.

3.2 HVAC system

In the following, the sub-models of the desiccant module, the AC evaporator and the radiator are presented.

3.2.1 Desiccant module

The dynamic model of the desiccant module is based on the LTT Adsorption Energy Systems Library [23]. The model consists of two control volumes, one for the air and one for the adsorption material. These control volumes are connected by models for heat and mass transfer.

For each control volume, the energy and the mass balance are solved. For air, the media model of humid air is used as described in the VDI guideline 4670: Thermodynamic properties of humid air and combustion gases [21] (cf. Section 3.1.2). For the adsorption material, a media model based on measurement data of Goldsworthy is used [24]. This model describes the water uptake of the adsorbent material based on the current temperature and the relative humidity of the air. As adsorbent material, AQSOA Z02 is used. AQSOA Z02 is a commercial adsorption material produced by Mitsubishi Plastics Inc. and is well suited for this application. Other adsorption materials, such as silica gels could also be used for this application.

The air volume and the adsorbent volume are connected by models for heat and mass transfer: Heat transfer is based on the temperature difference between air and adsorption material. The heat transfer coefficient describing the convective heat transfer between air and adsorbent particles depends on the air flow velocity and geometry of the particles [25]. Mass transfer is based on the Linear-Driving-Force approach with the partial pressure difference of water as the driving potential. The mass transfer coefficients are based on Hougen and Marshall [26].

The desiccant module is discretized in flow direction. The desiccant module itself is adiabatic, i.e. no heat losses to ambient air are considered. The model of the desiccant module has been validated experimentally [23].

3.2.2 AC-evaporator

For the AC-evaporator, the energy and mass balance of a single control volume are solved. As control parameter, the removed heat (and moisture when reaching 100% saturation) is used, i.e. the removed heat is an input to the AC-evaporator model. In

real AC-systems, the removed heat is controlled by the compressor displacement or speed and by the expansion valve diameter.

3.2.3 Radiator

For the radiator, again, the energy and mass balance of a single control volume are solved. For the radiator model, the heat flow rate is used as a model input. Since by the radiator model the air temperature can only be increased, the moisture content of the air stays constant.

Pressure losses throughout the HVAC system are neglected.

4 Results

As described in Section 2.2, three operating strategies are compared: (1) reference strategy (no air recirculation), (2) controlled air recirculation rate, and (3) desiccant-assisted controlled air recirculation rate. For operating strategies 2 and 3, the set-value of the relative windshield humidity is set to $\varphi_{\text{set,cabin}} = 80\%$. Thereby, a safe operation without the risk of fogging is ensured.

For the desiccant module, 1.3 kg of desiccant material are used. This amount of adsorption material allows adsorbing approximately the moisture provided by 2 persons for 2 h when using AQSOA Z02 as adsorption material. The used amount of adsorption material corresponds to a module size of ~ 1.85 l. Thus, a possible geometry of the module is 25 cm x 25 cm x 3 cm. In this study, the adsorption material is assumed to be a packed bed with a pellet diameter of 2 mm. With an air mass flow rate of 4 kg/min, this module configuration leads to pressure losses of ~ 5 mbar according to pressure loss correlations of a packed bed [25].

Given these model assumptions, the following simulation procedure is conducted to determine the energy demand for each operating strategies: A 2-hour ride is simulated where the initial temperature of all components equals the ambient temperature. Thus, no pre-conditioning of the cabin is assumed. Ambient temperatures between -20 °C and 10 °C are considered. The ambient humidity is set to $\varphi_{\text{ambient}} = 70\%$ for all cases. To determine the convective heat transfer coefficient on the outside, a constant vehicle speed of 33 km/h is used, which is the average speed of the NEFZ cycle. For the HVAC system, a constant total air mass flow rate of 4 kg/min in HVAC system is used and the desired cabin temperature is set to $T_{\text{set,cabin}} = 25$ °C [9].

To charge the desiccant module, an airflow of 3 kg/min is assumed which is heated to 90 °C. The water loading of the desiccant module at the start of the charging depends on the amount of water adsorbed during the ride, which in turn depends on the outside conditions and the number of passengers. Thus, the energy consumption needed for charging the desiccant module is based on the outside conditions and the number of passengers. For charging the battery, a charging efficiency of 90 % is

assumed according to measurements for different electrical vehicles reported by Tober [4].

Fig. 4 shows the electrical energy consumption for heating for the three operating strategies: (1) reference strategy with 0 % air recirculation rate (ARR), (2) controlled air recirculation rate, and (3) desiccant-assisted controlled air recirculation rate. Additionally, the electrical energy consumption due to charging losses of the battery and the electrical energy demand for charging desiccant module are shown. By adding the energy consumption needed for charging, we get the total electrical energy consumption for each operating strategy. Compared to the reference case, operating strategy 2 achieves only a slight reduction in energy consumption for ambient temperatures above $T_{\text{ambient}} = -10\text{ }^{\circ}\text{C}$: for $T_{\text{ambient}} = 0\text{ }^{\circ}\text{C}$, the electrical energy demand for heating can be reduced by 12 %. For $T_{\text{ambient}} = -20\text{ }^{\circ}\text{C}$, no difference in the energy consumption between strategy 1 and strategy 2 can be observed. Hence, the potential for recirculating the cabin air is small when using the set-up without the desiccant module.

When adding the desiccant module (operating strategy 3), significant reductions in electrical energy consumption for all ambient temperatures can be observed: for $T_{\text{ambient}} = 0\text{ }^{\circ}\text{C}$, the relative energy reduction exceeds 66 %. The active dehumidification allows high air recirculation rates which lead to the observed decrease in the electrical energy demand for heating.

To charge the desiccant module, around 0.5 kWh are necessary in all cases. This energy demand is more than compensated by the energy savings during the ride. Thus, the desiccant-assisted system is both beneficial during the ride, and in terms of overall efficiency. The overall energy efficiency of the desiccant-assisted system shows to be much better compared to the reference set-up.

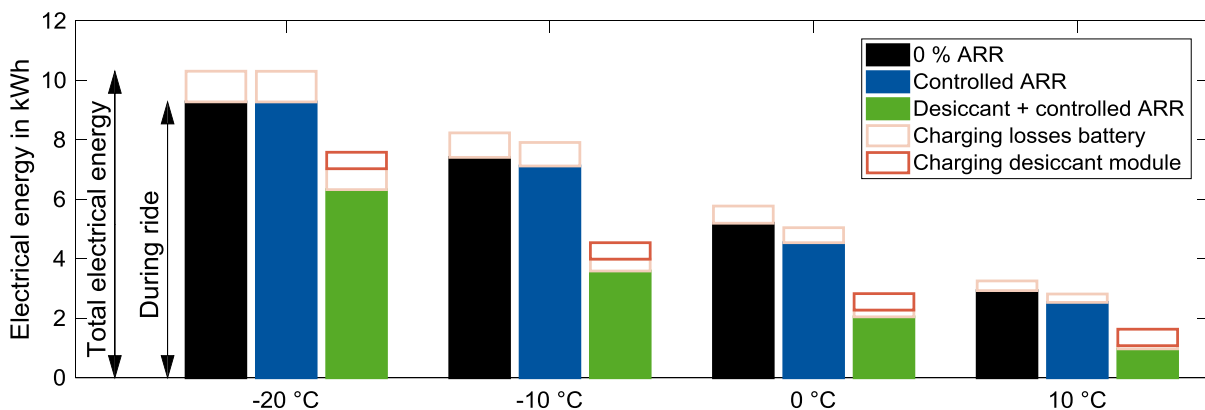


Fig. 4: Electrical energy demand for a 2 h ride at varying ambient temperatures for the three operating strategies: (1) reference strategy with 0 % air recirculation rate (ARR), (2) controlled air recirculation rate, and (3) desiccant-assisted controlled air recirculation rate. The additional electrical energy demand due to charging of the battery and the electrical energy demand for charging the desiccant module are also shown.

To visualise the achieved decrease in electrical energy consumed for heating, we define the share of electrical energy for driving/heating by:

$$\text{Share of electrical energy} = \frac{\text{Electrical energy for driving/heating}}{\text{driving} + \text{heating consumption}}$$

assuming an average speed of 33 km/h (NEFZ) and a constant average drivetrain consumption of 0.15 kWh/km.

Fig. 5 shows the share of electrical energy for the three operating strategies. For the desiccant-assisted set-up, heating has a smaller share for all ambient temperatures: the driving range suffers less when heating the cabin, while ensuring the same thermal comfort. For $T_{\text{ambient}} = -10\text{ }^{\circ}\text{C}$, the share of electrical energy available for driving increases from 56 % for the reference strategy to 73 % for the desiccant-assisted strategy. For $T_{\text{ambient}} = 0\text{ }^{\circ}\text{C}$, the share increases from 64 % to 82 %. These numbers show that the impact of cold temperatures on driving range can be significantly reduced by the desiccant-assisted heating concept.

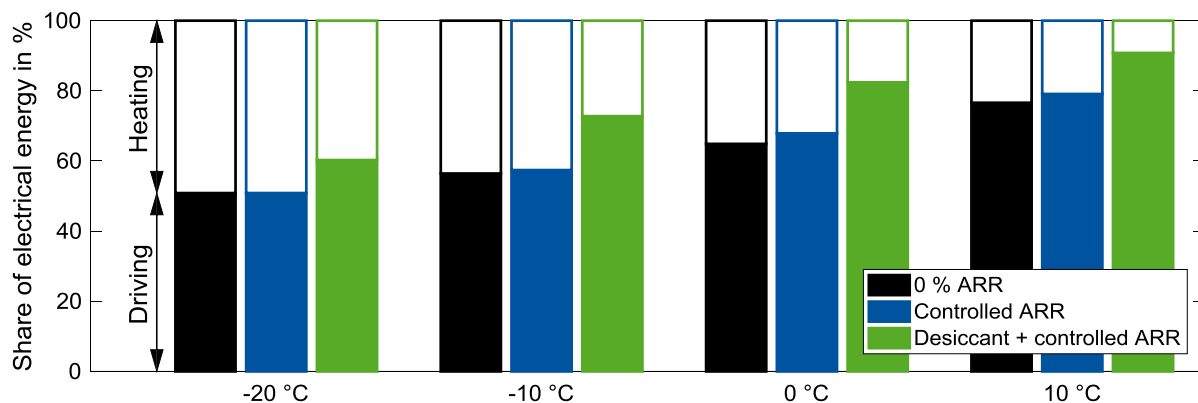


Fig. 5: Share of electrical energy used for driving/heating at varying ambient temperatures for the three operating strategies: (1) reference strategy with 0 % air recirculation rate (ARR), (2) controlled air recirculation rate, and (3) desiccant-assisted controlled air recirculation rate.

In the following, a detailed transient analysis for the case $T_{\text{ambient}} = -10\text{ }^{\circ}\text{C}$ is shown. The $T_{\text{ambient}} = -10\text{ }^{\circ}\text{C}$ case serves as an example to show the general effects. Similar results are obtained for the other ambient temperatures.

In Fig 6 left, the heat-up times are compared: The heat-up time is the time the cabin air needs to reach set temperature of $25\text{ }^{\circ}\text{C}$. This heat-up time can be reduced from 14 min for operating strategy 1 to 6 min for operating strategy 3 (desiccant-assisted with controlled air recirculation rate).

In Fig. 6 middle, the heat flow rates at the radiator are compared: For the desiccant-assisted operating strategy, the heating power is significantly reduced. After reaching $T_{\text{cabin}} = 25\text{ }^{\circ}\text{C}$, the heating power can be reduced to below 2 kW which is half the power as for operating strategy 1 and 2 (without desiccant module). Additionally, the maximum available heating power of 5 kW is not required for operating strategy 3.

Finally, the used air recirculation rates are compared in Fig 6 right: In operating strategy 1, the air recirculation rate is set to 0 %. For the controlled air recirculation rate (operating strategy 2), an air recirculation rate of 10-16 % is used after the first 5 min. For the desiccant-assisted operating strategy, the air recirculation rate rises to 100 % (from initial ARR = 0 %). The maximum air recirculation rate is used for 40 min. Afterwards, the ARR decreases slowly, since the desiccant module loses water adsorption capacity.

To sum up, the desiccant-assisted heating concept achieves shorter heat-up times while using less heating power.

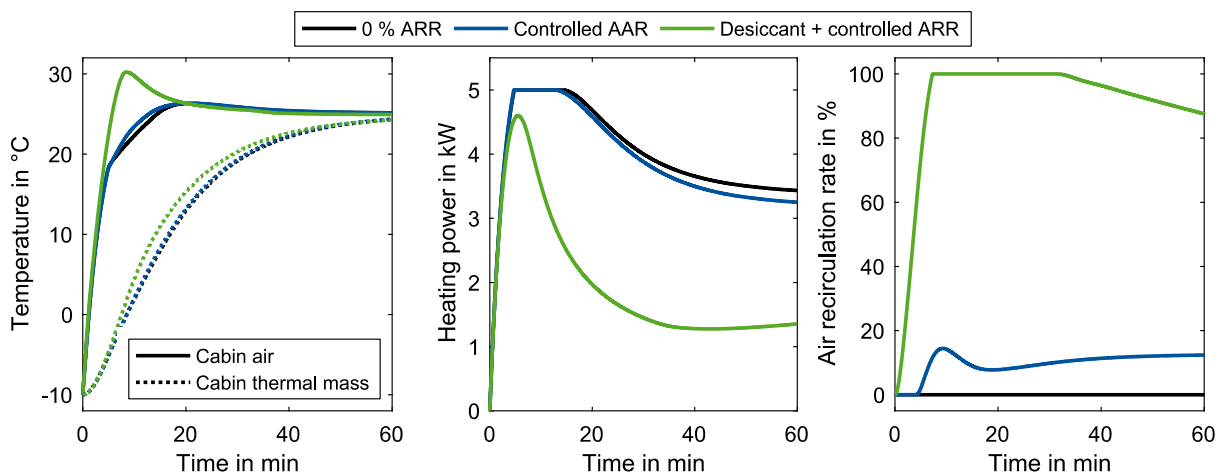


Fig. 6: Transient analysis for outdoor temperature of $-10\text{ }^{\circ}\text{C}$: Left: Temperature of cabin air and cabin thermal mass; Middle: Heating power to reach and hold set temperature of $T_{\text{set,cabin}} = 25\text{ }^{\circ}\text{C}$; Right: air recirculation rate while ensuring $\varphi_{\text{windshield}} < 80\text{ }%$.

5 Conclusions

A desiccant-assisted heating concept is proposed for battery-driven electric vehicles. It is shown that the desiccant-assisted concept allows significantly reducing the heating demand in winter. The desiccant-assisted system actively adsorbs water from the airflow which allows an increased air recirculation rate without windshield fogging. It is shown that a 1.3 kg module is sufficiently large to adsorb the moisture of 2 passengers for 2 hours. The desiccant-assisted set-up saves up to 66 % of electrical energy demand for heating compared to a conventional set-up using no air recirculation. The reduced heating demand allows significantly increasing the driving range in winter. Additionally, the overall energy demand combining the energy for driving and for charging is lowest for the desiccant-assisted set-up. Moreover, at the beginning of a ride, the desiccant-assisted set-up speeds up cabin heating: for the case $T_{\text{ambient}} = -10\text{ }^{\circ}\text{C}$, the time to reach the cabin set temperature of $25\text{ }^{\circ}\text{C}$ can be reduced from 14 to 6 minutes. In summary, the proposed desiccant-assisted heating concept seems highly promising and experimental implementation of the concept is very desirable.

6 References

- [1] International Energy Agency
Global EV Outlook 2016: Beyond one million electric cars
OECD/IEA
Paris, 2016
- [2] ENTHALER, A.; WEUSTENFELD, T.; GAUTERIN, F.; KÖHLER, J.
Thermal management consumption and its effect on remaining range estimation of electric vehicles
International Conference on Connected Vehicles and Expo (ICCVE)
Vienna, 2014, pp. 170-177
- [3] AHMED, N.K.; KAPADIA, J.
Seasonality Effect on Electric Vehicle Miles Traveled in Electrified Vehicles
SAE International Journal of Alternative Powertrains
2017, 6(1), pp. 47-53
- [4] TOBER, W.
Praxisbericht Elektromobilität und Verbrennungsmotor
Springer Vieweg
Wiesbaden, 2016
- [5] AUER, M.
Ein Beitrag zur Erhöhung der Reichweite eines batterieelektrischen Fahrzeugs durch prädiktives Thermomanagement
Springer Vieweg
Wiesbaden, 2016
- [6] CHRISTEN, E.J.; BLATCHLEY, T.; JACOBSON, M.; AHMED, N.K.; GONG, Q.
Improving Range Robustness. Heat Pump Value for Plug-In Electric Vehicles
WCX™ 17: SAE World Congress Experience
Warrendale, PA, 2017
- [7] LAJUNEN, A.
Energy Efficiency and Performance of Cabin Thermal Management in Electric Vehicles
WCX™ 17: SAE World Congress Experience
Warrendale, PA, 2017
- [8] TITOV, G.; LUSTBADER, J.A.
Modeling Control Strategies and Range Impacts for Electric Vehicle Integrated Thermal Management Systems with MATLAB/Simulink
WCX™ 17: SAE World Congress Experience
Warrendale, PA, 2017

- [9] GROßMANN, H.
PKW-Klimatisierung: Einführung in physikalische Grundlagen
5. VDI-Fachkonferenz. Thermomanagement für elektromotorisch angetriebene PKW
Stuttgart, 2016
- [10] BRÈQUE, F.; NEMER, M.
Cabin Thermal Needs: Modeling and Assumption Analysis
Proceedings of the 12th International Modelica Conference
Prague, 2017, pp. 771-781
- [11] LORENZ, M.; FIALA, D.; SPINLER, M.; SATTELMAYER, T.
A Coupled Numerical Model to Predict Heat Transfer and Passenger Thermal Comfort in Vehicle Cabins
SAE 2014 World Congress & Exhibition
Warrendale, PA, 2014
- [12] MASSONET, C.; PINGEL, M.; BACKES, D.
Aufbau und Anwendung eines elektrischen Heiztextilsystems zur Steigerung des Innenraumkomforts
5. VDI-Fachkonferenz. Thermomanagement für elektromotorisch angetriebene PKW
Stuttgart, 2016
- [13] NIELSEN, F.; UDDHEIM, Å.; DALENBÄCK, J.-O.
Reduction of Energy Used for Vehicle Interior Climate
SAE 2016 World Congress and Exhibition
Warrendale, PA, 2016
- [14] NAGANO, H.; TOMITA, K.; TANOUE, Y.; KOBAYASHI, Y.; KOHRI, I.; KATO, S.
Analysis of Defogging Pattern on Windshield and Ventilation Load Reduction based on Humidity Distribution Control
SAE 2016 World Congress and Exhibition
Warrendale, PA, 2016
- [15] OIWAKE, M.; YOSHIICHI, O.; OBATA, S.; NAGANO, H.; KOHRI, I.
Effects of the Glass and Body Heat Transfer Characteristics of a Hybrid Electric Vehicle on Its Fuel Consumption and Cruising Distance
WCX™ 17: SAE World Congress Experience
Warrendale, PA, 2017
- [16] ATKINSON, W.J.; HILL, W.R.; MATHUR, G.D.
The Impact of Increased Air Recirculation on Interior Cabin Air Quality
WCX™ 17: SAE World Congress Experience
Warrendale, PA, 2017

- [17] LINDEMANN, A.; SAUER, D.U.; SCHÄPER, C.; WAWZYNIAK, M.; WIEBELT, A.
Energiemanagement und Regelung - Die Elektrifizierung des Antriebsstrangs
Springer Vieweg
Wiesbaden, 2015, pp. 78-102
- [18] BAU, U.; SCHREIBER, H.; LANZERATH, F.; BARDOW, A.
Hybride Klimatisierung für Elektrofahrzeuge: Kombination von Wärmepumpe
und offenem Sorptionssystem - Wärmemanagement des Kraftfahrzeugs X
expert-Verlag
Potsdam, 2016
- [19] International Organization for Standardization (ISO)
ISO 12837, Road vehicles — Safety glazing materials — Method for the
determination of solar transmittance
Geneva, 2008
- [20] VDI-Wärmeatlas
Springer Vieweg
Berlin, 2013
- [21] Verein Deutscher Ingenieure (VDI)
VDI 4670, Thermodynamic properties of humid air and combustion gases
Beuth Verlag
Berlin, 2016
- [22] Verein Deutscher Ingenieure (VDI)
VDI 2078, Berechnung der thermischen Lasten und Raumtemperaturen
(Auslegung Kühllast und Jahressimulation)
Beuth Verlag
Berlin, 2015
- [23] BAU, U.; LANZERATH, F.; GRÄBER, M.; SCHREIBER, H.; THIELEN, N.;
BARDOW, A.
Adsorption energy systems library - Modeling adsorption based chillers, heat
pumps, thermal storages and desiccant systems
Proceedings of the 10th International Modelica Conference
Lund, 2014, pp. 875-883
- [24] GOLDSWORTHY, M.J.
Measurements of water vapour sorption isotherms for RD silica gel, AQSOA-
Z01, AQSOA-Z02, AQSOA-Z05 and CECA zeolite 3A
Microporous and Mesoporous Materials
2014, (196), pp. 59-67

- [25] KAST, W.
Adsorption aus der Gasphase ingenieurwissenschaftliche Grundlagen und technische Verfahren
Wiley-VCH
Weinheim 1988
- [26] HOUGEN, O.A.; MARSHALL, W.R.
Adsorption from a fluid stream flowing through a stationary granular bed
Chem. Eng. Prog.
1947, (43), pp. 197-208